

Gauge-Higgs Unification in Orbifold Models

C. A. Scrucca^a, M. Serone^b, L. Silvestrini^c, A. Wulzer^b

^a*Theor. Phys. Div., CERN, CH-1211 Geneva 23, Switzerland*

^b*ISAS-SISSA and INFN, Via Beirut 2-4, I-34013 Trieste, Italy*

^c*INFN, Sez. di Roma, Dip. di Fisica, Univ. di Roma "La Sapienza"
P.le Aldo Moro 2, I-00185, Rome, Italy*

Abstract

Six-dimensional orbifold models where the Higgs field is identified with some internal component of a gauge field are considered. We classify all possible T^2/\mathbf{Z}_N orbifold constructions based on a $SU(3)$ electroweak gauge symmetry. Depending on the orbifold twist, models with two, one or zero Higgs doublets can be obtained. Models with one Higgs doublet are particularly interesting, as they lead to a prediction for the Higgs mass that is twice the W boson mass at leading order: $m_H = 2m_W$. The electroweak scale is quadratically sensitive to the cut-off, but only through very specific localized operators. We study in detail the structure of these operators at one loop, and identify a class of models where they do not destabilize the electroweak scale at the leading order. This provides a very promising framework to construct realistic and predictive models of electroweak symmetry breaking.

1. Introduction

If the Standard Model (SM) is seen as a low-energy effective description of a more fundamental theory valid up to a scale Λ , the order of magnitude of the Higgs mass m_H , as suggested by global fits of electroweak precision data, is natural only if one assumes a quite low scale for Λ . Taking as a reference value $m_H \sim 100$ GeV and requiring this to be the magnitude of the leading one-loop correction from the Yukawa coupling to the top quark, $\delta m_H \sim \frac{\sqrt{3}}{2\pi} |\lambda_t| \Lambda$, one finds $\Lambda \sim 400$ GeV. On the other hand, in order to respect the stringent bounds from electroweak precision physics, Λ should be much higher than that. Present bounds from generic four-fermion operators with coefficients of order Λ^{-2} require Λ to be at least 5 – 10 TeV (see *e.g.* [1]). This discrepancy of more than one order of magnitude between the natural value of Λ and its experimental lower bound defines the little hierarchy problem, and can be interpreted as a measure of the amount of fine-tuning that is required for a generic extension of the SM. Its present value of about 5 – 10 % poses a significant theoretical problem, which is known to affect also the most promising scenario of physics beyond the SM, namely Supersymmetry (SUSY). This strongly motivates the investigation of other possible scenarios which could solve this little hierarchy problem.

The idea that the SM Higgs field might be an internal component of a gauge field of an extended electroweak symmetry, propagating in more than four dimensions, is particularly appealing in the above context, because it allows to build models where the electroweak symmetry breaking (EWSB) scale is stabilized thanks to the higher-dimensional gauge symmetry. This idea of gauge–Higgs unification was proposed long ago [2], and recently received renewed interest, in both its non-SUSY [3]–[7] and SUSY [8] versions. The simplest framework allowing its implementation is a five-dimensional ($5D$) $SU(3)$ gauge theory on an S^1/\mathbf{Z}_2 orbifold [9]. This model presents many interesting features, but it predicts, in its minimal version, too low values for the Higgs mass (see [7] for a detailed study of these models), because of the absence of any tree-level Higgs potential, a common feature of all $5D$ models with a single Higgs doublet.¹

New features emerge when applying the above ideas in the presence of two or more extra dimensions.² First, the gauge kinetic term contains in its non-abelian part a quartic potential for the internal components of the gauge field, and thus for the Higgs fields [4]. This opens the possibility of increasing the Higgs mass to acceptable values. Second, the gauge symmetry allows for the appearance of an operator, localized at the orbifold fixed points, that is proportional to the internal

¹In $5D$ SUSY models, a tree-level Higgs potential can occur, but at the price of having at least two Higgs doublets.

² $D > 5$ orbifolds also present new possibilities in the context of flavour physics, see *e.g.* ref. [10].

component of the gauge field strength in the hypercharge direction and contains a mass term for the Higgs fields in its non-abelian part [6, 11]. These tadpoles are generated with quadratically divergent coefficients and can unfortunately destabilize the EWSB scale. In supersymmetric models, they correspond to localized Fayet–Iliopoulos (FI) terms, since the $4D$ vector auxiliary field D is identified with its $6D$ counterpart shifted by the internal components of the gauge field strength [12].

In the light of the above remarks, it is of primary importance to understand whether and to what extent the idea of gauge–Higgs unification can be implemented with qualitative success in $D > 5$ dimensions, before attempting to build a realistic model. One more drawback of $D > 5$ models with respect to $D = 5$ models, besides the possible occurrence of quadratic divergences, is some loss of predictivity. Indeed, there are typically more geometric moduli, parametrizing the shape and size of the internal space, and also more Higgs fields, since there are more internal dimensions. The simplest model of gauge–Higgs unification in $6D$ can be obtained by considering an $SU(3)$ gauge theory on a T^2/\mathbf{Z}_2 orbifold [5], and gives rise to three geometric moduli and two Higgs doublets. In this model, there turns out to be a parity symmetry that can forbid the appearance of the divergent tadpole, or allow to control its size through some parameter if it is softly broken. The Higgs potential in this model has the same structure as that of the Minimal Supersymmetric Standard Model (MSSM) and it seems again difficult to get reasonable masses for all the Higgs fields after the EWSB.

The aim of this paper is to explore all $6D$ toroidal orbifold constructions of the form T^2/\mathbf{Z}_N (with $N = 2, 3, 4, 6$), giving rise to $6D$ gauge–Higgs unification without SUSY. We mainly focus on the minimal $SU(3)$ unified gauge symmetry, which is broken to the SM $SU(2) \times U(1)$ EW symmetry by the orbifold projection, one or more Higgs fields being responsible for EWSB.³ Differently from the $N = 2$ model, which necessarily leads to two Higgs doublets, $N > 2$ models offer more possibilities and can lead for instance to a single Higgs doublet. Interestingly, in contrast to the $5D$ case, one also gets a non-vanishing tree-level quartic coupling, given by the usual gauge coupling. Under the assumption that EWSB occurs, the Higgs mass in these models is therefore predicted to be twice the W mass at tree-level:

$$m_H = 2 m_W . \tag{1.1}$$

For these $N > 2$ models, however, there seems to exist no symmetry able to forbid the localized divergent tadpole, and the electroweak scale is therefore expected to be unstable.

³See [13] for the possibility of constructing Higgsless theories where EWSB is achieved by boundary conditions and unitarity breaking occurs at scales higher than m_Z .

In the following, we present an explicit one-loop computation of the tadpole coefficients and show that the corresponding operator is indeed radiatively generated at the orbifold fixed points. We study in detail the contributions of scalar, spinor and vector fields, and show that even an accidental cancellation at each fixed point seems impossible without introducing fundamental scalars. On the other hand, the integral of the tadpole over the compact space can happen to vanish. In this case, one can expect that its presence should not affect the mass of the Higgs field, as happens for a globally vanishing FI term in 5D SUSY models [14]. A complete analysis of the effects of general localized tadpoles on the wave functions and on the spectrum of the Higgs modes is not totally straightforward. Fortunately, the case of a globally vanishing tadpole can be analysed along the lines of [15] for the SUSY case. It turns out that a globally vanishing tadpole induces a non-trivial gauge-field background that does not give rise to EWSB and in which there indeed exists a zero-mode for the Higgs field. Its wave function has a non-trivial profile along the compact space and displays localization or delocalization at the fixed points, in complete analogy with SUSY theories with localized FI terms [15].

We believe that higher-dimensional orbifold constructions of this type, with a single Higgs field, a tree-level quartic potential and a vanishing integrated tadpole at the one-loop level, represent an extremely promising class of models. EWSB can be induced by finite radiative corrections to the Higgs mass term, associated to non-local operators, which we compute in the following, and is stable at the one-loop level. A direct sensitivity of the EW scale to the cut-off can only arise at two loops, and the little hierarchy problem is solved.

The paper is organized as follows. In section 2 we introduce the T^2/\mathbf{Z}_N orbifolds and analyse the possible 4D field configurations that can be obtained. In section 3 the classical and quantum forms of the Higgs potential are studied. In section 4 we compute the contributions of bulk gauge fields, as well as scalars and fermions in arbitrary representations, to the divergent localized tadpole. Finally, section 5 contains a discussion of the effect induced by the tadpole and general phenomenological implications.

2. Orbifold models in six dimensions

Let us consider a 6D gauge theory compactified on the orbifold T^2/\mathbf{Z}_N . The 2D torus is parametrized by three real parameters, the two radii R_1 and R_2 and an angle θ , and is defined by identifying points in a plane as

$$\begin{aligned} y^1 &\sim y^1 + n 2\pi R_1 + m 2\pi R_2 \cos \theta, \\ y^2 &\sim y^2 + m 2\pi R_2 \sin \theta, \end{aligned} \tag{2.1}$$

for any integers m, n . It is useful to introduce complex coordinates $z = \frac{1}{\sqrt{2}}(y^1 + iy^2)$, so that the metric components⁴ with $A, B = z, \bar{z}$ are given by $g_{z\bar{z}} = g^{\bar{z}z} = -1$. Defining the modular parameter $U = \frac{R_2}{R_1}e^{i\theta}$, and renaming $R \equiv R_1$, the lattice (2.1) can then be rewritten in the complex plane as

$$z \sim z + (m + nU)\frac{2\pi R}{\sqrt{2}}. \quad (2.2)$$

The generator g of the orbifold group \mathbf{Z}_N acts on the torus as a $\frac{2\pi}{N}$ rotation. Consistent orbifold constructions are constrained by the possible crystallographic symmetries of $2D$ lattices. They exist only for $N = 2$ with arbitrary U and for $N = 3, 4, 6$ with $U = e^{\frac{2\pi i}{N}}$ or other equivalent discrete choices. This means that for $N = 3, 4, 6$ there is only one Kähler modulus parametrized by R , as in the $5D$ model on S^1/\mathbf{Z}_2 , whereas in the degenerate case $N = 2$ there is in addition a complex structure modulus U . The orbifold generator acts on the coordinates as $z \rightarrow \tau z$, with $\tau = e^{\frac{2\pi i}{N}}$, and is also embedded into the gauge group through a matrix P such that $P^N = 1$. For simplicity, we consider only group actions in the gauge sector that correspond to inner automorphisms of the gauge group G (see *e.g.* [16] for a discussion of various orbifold gauge actions), in which $P \in G$ (up to a constant overall phase for matter fields).

The Lagrangian of the orbifold theory is constrained to be the sum of a bulk contribution, which must be invariant under the full gauge group, and a set of contributions localized at the fixed points of the orbifold action, which have to be invariant only under the gauge group surviving at these points. The set of points left fixed by an element g^k of the orbifold group depends on $k = 0, 1, \dots, N-1$, and it is therefore necessary to distinguish sectors labelled by different k . Since g^{N-k} is the inverse of g^k , the fixed points in the sectors k and $N-k$ are the same, and their number is given by

$$N_k = \left[2 \sin \left(\frac{\pi k}{N} \right) \right]^2. \quad (2.3)$$

Moreover, the sector $k = 0$ is trivial and has of course no fixed points. The physically distinct and relevant sectors are therefore labelled by $k = 1, \dots, [N/2]$, where $[\dots]$ denotes the integer part. The general form of the effective Lagrangian can therefore be parametrized as

$$\mathcal{L} = \mathcal{L}_6 + \sum_{k=1}^{[N/2]} \sum_{i_k=1}^{N_k} \delta^{(2)}(z - z_{i_k}) \mathcal{L}_{4, i_k}, \quad (2.4)$$

where \mathcal{L}_6 represents the bulk $6D$ Lagrangian and \mathcal{L}_{4, i_k} the localized Lagrangians at the N_k g^k fixed points. Since \mathcal{L} has to be g -invariant, and g acts non-trivially

⁴Our convention for the $6D$ metric is mostly minus.

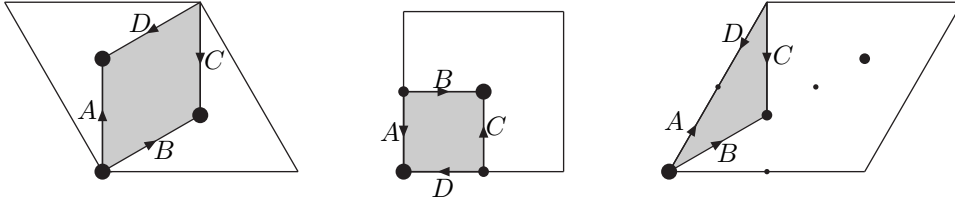


Figure 1: From left to right, the T^2/\mathbf{Z}_3 , T^2/\mathbf{Z}_4 and T^2/\mathbf{Z}_6 orbifolds and their covering tori. We indicate with points of decreasing size the g , g^2 and g^3 fixed points respectively. The grey region represents the fundamental domain of the orbifolds, and the segments delimiting it must be identified according to: $A \sim D$, $B \sim C$.

on some fixed points, there are in general various non-trivial constraints among the \mathcal{L}_{4,i_k} 's. Moreover, the orbifold structure respects a discrete translational symmetry mapping g fixed points onto g fixed points.⁵ This implies that the Lagrangians \mathcal{L}_{4,i_k} are constrained to be all equal at fixed k and hence there are only $[N/2]$ independent localized terms appearing in (2.4).

Contrary to the more familiar cases of the \mathbf{Z}_2 and \mathbf{Z}_3 orbifolds, for the \mathbf{Z}_4 and \mathbf{Z}_6 orbifolds there are points that are fixed under the action of some element g^k of the group, but not fixed under some subgroup of \mathbf{Z}_N , which permutes them. From eq. (2.3) one finds that the \mathbf{Z}_4 orbifold has two g (and g^3) fixed points and four g^2 fixed points: the two g fixed points, and two more points that are exchanged by the action of g . The \mathbf{Z}_6 orbifold has one g (and g^5) fixed point, the origin $z = 0$, three g^2 and four g^3 fixed points. Besides $z = 0$, the remaining two g^2 fixed points are exchanged by the action of g^3 , whereas the remaining three g^3 fixed points are exchanged by the action of g^2 . We summarize in Fig. 1 the orbifold fixed-point structure of the \mathbf{Z}_3 , \mathbf{Z}_4 and \mathbf{Z}_6 orbifolds, leaving aside the more familiar \mathbf{Z}_2 case.

In the following we shall restrict our study to the prototype models of gauge-Higgs unification with a gauge group $G = SU(3)$ that is broken to $H = SU(2) \times U(1)$ by the \mathbf{Z}_N orbifold projection. We denote by t^a the $SU(3)$ generators with the standard normalization $\text{Tr } t^a t^b = \frac{1}{2} \delta^{ab}$ in the fundamental representation. The unbroken generators in $SU(2)$ and $U(1)$ are $t^{1,2,3}$ and t^8 . The broken generators in $SU(3)/[SU(2) \times U(1)]$ are instead $t^{4,5,6,7}$, and can be conveniently grouped into the usual raising and lowering combinations $t^{\pm 1} = \frac{1}{\sqrt{2}}(t^4 \pm it^5)$ and $t^{\pm 2} = \frac{1}{\sqrt{2}}(t^6 \pm it^7)$. In this basis, the group metric in the sector $\pm i, \pm j$ is given by $h_{+i,-j} = h^{+i,-j} = \delta^{ij}$. The most general way to realize the above breaking is obtained by embedding the

⁵This is true only in the absence of localized matter that is not uniformly distributed over the fixed points or of discrete Wilson lines.

orbifold twist in the gauge group through the matrix

$$P = \tau^{2n_p(\frac{1}{3} + \frac{1}{\sqrt{3}}t^8)} = \begin{pmatrix} \tau^{n_p} & 0 & 0 \\ 0 & \tau^{n_p} & 0 \\ 0 & 0 & 1 \end{pmatrix}. \quad (2.5)$$

The number n_p must be an integer and is defined only modulo N , so that there are a priori $N - 1$ inequivalent embeddings.

The geometric part of the \mathbf{Z}_N action on a field is fixed by the decomposition of its representation under the $6D$ $SO(1, 5)$ Lorentz group in terms of $SO(1, 3) \times SO(2)$, where $SO(1, 3)$ is the $4D$ Lorentz group and $SO(2) \simeq U(1)$ is the group of internal rotations. The gauge part of the action on a field in a representation \mathcal{R} of $SU(3)$ is instead given by the twist matrix (2.5) generalized to the representation \mathcal{R} . This fixes the \mathbf{Z}_N properties of any field, up to an arbitrary overall phase g , such that the N -th power of the \mathbf{Z}_N action is trivial on all the components of the field. The orbifold boundary condition of a generic bosonic or fermionic field component Φ , with $U(1)$ charge s under internal rotations and in the representation \mathcal{R} of $SU(3)$, is then given by⁶

$$\Phi(\tau z) = g_{B,F} R_s P_{\mathcal{R}} \Phi(z). \quad (2.6)$$

In this equation, $P_{\mathcal{R}}$ denotes the twist matrix P in the representation \mathcal{R} and $R_s = \tau^s$ is the Lorentz rotation associated to the geometric action of the twist. The overall phases $g_{B,F}$ are such that $g_B^N = 1$ for bosons and $g_F^N = -1$ for fermions, since $R_s^N = \pm 1$ in the two cases. It is convenient to define $g_F = g\tau^{\frac{1}{2}}$, $g_B = g$, so that g is an N -th root of unity for both bosons and fermions. Correspondingly, there are in general N different boundary conditions, associated to the N possible choices of g . They are the \mathbf{Z}_N analogues of the more familiar even and odd parities appearing in \mathbf{Z}_2 models.

The expression of $P_{\mathcal{R}}$ can be conveniently written as

$$P_{\mathcal{R}} = \tau^{2n_p(\frac{n_{\mathcal{R}}}{3} + \frac{1}{\sqrt{3}}t_{\mathcal{R}}^8)}, \quad (2.7)$$

where $t_{\mathcal{R}}^8$ is the Cartan generator t^8 in the representation \mathcal{R} and $n_{\mathcal{R}}$ is an integer number such that $P_{\mathcal{R}}^N = 1$. It can be written as $n_{\mathcal{R}} = n_1 - n_2$, where n_1 and n_2 are the two Dynkin labels of the representation \mathcal{R} . Since the canonically normalized abelian generator surviving the projection is $Q_{\mathcal{R}} = \frac{1}{\sqrt{3}}t_{\mathcal{R}}^8$, the matrix (2.7) gives a phase $\tau^{2n_p(\frac{n_{\mathcal{R}}}{3} + q)}$ on a component with $U(1)$ charge q under the decomposition of the representation \mathcal{R} under $SU(3) \rightarrow SU(2) \times U(1)$. The relevant information is listed in Table 1 for the first few representations. In the following two subsections, we consider in some more detail the decomposition of gauge and matter fields, as given by (2.6).

⁶Here and in the following, for simplicity, we do not explicitly indicate the dependence on \bar{z} and on the $4D$ coordinates x^μ .

\mathcal{R}	Decomposition of \mathcal{R}	$n_{\mathcal{R}}$
3	$\mathbf{2}_{\frac{1}{6}} \oplus \mathbf{1}_{-\frac{1}{3}}$	1
6	$\mathbf{3}_{\frac{1}{3}} \oplus \mathbf{2}_{-\frac{1}{6}} \oplus \mathbf{1}_{-\frac{2}{3}}$	2
8	$\mathbf{3}_0 \oplus \mathbf{2}_{\frac{1}{2}} \oplus \mathbf{2}_{-\frac{1}{2}} \oplus \mathbf{1}_0$	0
10	$\mathbf{4}_{\frac{1}{2}} \oplus \mathbf{3}_0 \oplus \mathbf{2}_{-\frac{1}{2}} \oplus \mathbf{1}_{-1}$	3

Table 1: Decomposition of the most relevant $SU(3)$ representations.

2.1. Gauge fields

The gauge fields A_M transform as vectors under $SO(1, 5)$ rotations and in the adjoint representation under gauge transformations. In complex coordinates, the decomposition of A_M under $SO(1, 3) \times U(1)$ is very simple: we get a $4D$ vector field A_μ with charge $s = 0$ and two $4D$ scalars A_z and $A_{\bar{z}}$ with charges $s = -1$ and $s = 1$ respectively. The boundary conditions can be obtained from eq. (2.6) with $g = 1$. The gauge part of the orbifold twist is diagonal if one switches from the standard basis with components A_{Ma} to the creation–annihilation basis with components $A_{M1,2,3,8}$, $A_{M\pm 1} = \frac{1}{\sqrt{2}}(A_{M4} \mp iA_{M5})$ and $A_{M\pm 2} = \frac{1}{\sqrt{2}}(A_{M6} \mp iA_{M7})$. The final result is that the various components of the gauge field $A_M = \sum_a A_{Ma} t^a$ satisfy twisted boundary conditions with the following phases:

$$A_{\mu 1,2,3,8} : 1, \quad A_{z 1,2,3,8} : \tau^{-1}, \quad A_{\bar{z} 1,2,3,8} : \tau^{+1}, \quad (2.8)$$

$$A_{\mu \pm i} : \tau^{\pm n_p}, \quad A_{z \pm i} : \tau^{-1 \pm n_p}, \quad A_{\bar{z} \pm i} : \tau^{+1 \pm n_p}. \quad (2.9)$$

The light modes of untwisted fields consist of the gauge bosons $A_{\mu 1,2,3,8}$ forming the adjoint of the surviving gauge group, the scalar fields A_{z+i} with their complex conjugates $A_{\bar{z}-i}$ forming a charged Higgs doublet under this group if $n_p = 1 \pmod N$, and the scalar fields A_{z-i} with their complex conjugate $A_{\bar{z}+i}$ forming a conjugate charged Higgs doublet if $n_p = -1 \pmod N$. Referring to the decomposition reported in Table 1, the projection keeps the $\mathbf{3}_0$ and $\mathbf{1}_0$ components for $4D$ indices and some numbers n and n_c of the $\mathbf{2}_{\frac{1}{2}}$ and the $\bar{\mathbf{2}}_{-\frac{1}{2}}$ components for internal indices, depending on N and $n_p = 1, \dots, N-1$. The possibilities for the numbers (n, n_c) for the consistent constructions labelled by the integers (N, n_p) are the following:

$$(n, n_c) = (1, 1) : \text{for } (N, n_p) = (2, 1); \quad (2.10)$$

$$(n, n_c) = (1, 0) : \text{for } (N, n_p) = (3, 1), (4, 1), (6, 1); \quad (2.11)$$

$$(n, n_c) = (0, 1) : \text{for } (N, n_p) = (3, 2), (4, 3), (6, 5); \quad (2.12)$$

$$(n, n_c) = (0, 0) : \text{for } (N, n_p) = (4, 2), (6, 2), (6, 3), (6, 4). \quad (2.13)$$

It is therefore possible to construct models with two conjugate Higgs doublets (\mathbf{Z}_2),

a single Higgs doublet $(\mathbf{Z}_3, \mathbf{Z}_4, \mathbf{Z}_6)$ or no Higgs doublets at all $(\mathbf{Z}_4, \mathbf{Z}_6)$.

2.2. Matter fields

A $6D$ Weyl fermion Ψ_{\pm} of definite $6D$ chirality decomposes under $SO(1, 3) \times U(1)$ into two $4D$ chiral fermions with charges $s = \pm\frac{1}{2}$: $\Psi_{\pm} = (\psi_{L,R})_{s=\frac{1}{2}} \oplus (\chi_{R,L})_{s=-\frac{1}{2}}$, where L, R denote the $4D$ chiralities. We thus see from (2.6) that any $6D$ Weyl spinor gives rise to two $4D$ fermions of opposite $4D$ chiralities, twisted by g and $g\tau$, times the gauge part of the twist. More generally, a $6D$ spinor field $\Psi_{\mathcal{R},\chi_6}$ of $6D$ chirality $\chi_6 = \pm 1$ transforming in a representation \mathcal{R} of the gauge group, gives rise to different $4D$ spinor components ψ_{q,χ_4} with $U(1)$ charge q and $4D$ chirality $\chi_4 = \pm 1$, twisted by a phase:

$$\psi_{q,\chi_4} : g \tau^{\frac{1-\chi_4\chi_6}{2}} \tau^{2n_p(\frac{n_{\mathcal{R}}}{3}+q)}. \quad (2.14)$$

Depending on N and n_p , the various possible choices for g allow the zero modes of different subsets of components to be preserved. We will not list here the many possibilities, since they can be easily derived from the data reported in Table 1.

For scalar fields the analysis is simpler, since they are singlets under Lorentz transformations and thus $s = 0$ in (2.6). The twist of a scalar field $\phi_{\mathcal{R}}$ in a representation \mathcal{R} of the gauge group is only given by its gauge decomposition. For a generic component ϕ_q with $U(1)$ charge q , one has

$$\phi_{\mathcal{R},q} : g \tau^{2n_p(\frac{n_{\mathcal{R}}}{3}+q)}. \quad (2.15)$$

Notice that there is a one-to-one correspondence between the case of scalars and that of spinors, since the additional phase $\tau^{\frac{1-\chi_4\chi_6}{2}}$ arising for the latter is always an N -th root of unity and can therefore be compensated by a different choice of g . It is easy to verify that the zero mode of any component can always be preserved with a suitable and unique choice of the phase g , both for scalars and for fermions. This is an important property for model building.

2.3. Wave functions and spectrum

To construct wave functions, it is convenient to introduce two alternative real coordinates w_1 and w_2 , which are aligned with the natural cycles specified by the complex structure $U = U_1 + iU_2$ and defined by the relation $z = \frac{1}{\sqrt{2}}(w_1 + U w_2)$. In this way, w_1 and w_2 are independently periodic with period $2\pi R$. For $N = 3, 4, 6$, where $U = \tau$, the \mathbf{Z}_N twist changes the point (w_1, w_2) into the point $(-w_2, w_1 + 2\tau_1 w_2)$, where $\tau_{1,2}$ denotes the real and imaginary parts of τ . For \mathbf{Z}_2 , one has simply $(w_1, w_2) \rightarrow \tau(w_1, w_2)$. It will be convenient in the following to introduce a matrix notation, in which the vector \vec{w} is transformed into the vector $Z_N^t \vec{w}$. The matrix Z_N is given by

$$Z_N = \begin{pmatrix} 0 & 1 \\ -1 & 2\tau_1 \end{pmatrix} \quad (2.16)$$

for $N = 3, 4, 6$, while $Z_2 = -I$. The basis of periodic functions on T^2 is then given by the usual exponential functions $f_{\vec{n}}(\vec{w}) \sim e^{\frac{i}{R}\vec{n}\cdot\vec{w}}$. In terms of the complex variable z , the normalized result is

$$f_{\vec{n}}(z) = \frac{1}{\sqrt{V}} e^{\frac{1}{\sqrt{2}}(\lambda_{\vec{n}}z - \bar{\lambda}_{\vec{n}}\bar{z})}, \quad (2.17)$$

where V is the volume of the covering torus and

$$\lambda_{\vec{n}} = \frac{n_2 - n_1\bar{U}}{U_2 R}, \quad \bar{\lambda}_{\vec{n}} = \frac{n_2 - n_1U}{U_2 R}. \quad (2.18)$$

The \mathbf{Z}_N twist acts on $f_{\vec{n}}$ and $\lambda_{\vec{n}}$ as

$$f_{\vec{n}}(\tau^k z) = f_{Z_N^k \vec{n}}(z), \quad \lambda_{Z_N^k \vec{n}} = \tau^k \lambda_{\vec{n}}. \quad (2.19)$$

It is easy to construct \mathbf{Z}_N covariant wave functions on T^2 by applying to the functions (2.17) the orbifold projection weighted by an arbitrary \mathbf{Z}_N phase g . Defining for convenience the quantity $\eta_{\vec{n}} = (\sqrt{N})^{-\delta_{\vec{n},\vec{0}}}$, these are given by

$$h_{\vec{n}}^g(z) = \frac{\eta_{\vec{n}}}{\sqrt{N}} \sum_{k=0}^{N-1} g^{-k} f_{Z_N^k \vec{n}}(z), \quad (2.20)$$

and, thanks to (2.19), satisfy the generic twisted boundary condition $h_{\vec{n}}^g(\tau z) = g h_{\vec{n}}^g(z)$. It is easy to verify that these functions are also orthonormal with respect to the Kaluza–Klein (KK) momenta as well as the twist g . However, the functions $h_{\vec{n}}^g(z)$ are not all independent: those with mode vectors connected by the orbifold action are proportional to each other through a phase:

$$h_{Z_N^k \vec{n}}^g(z) = g^k h_{\vec{n}}^g(z). \quad (2.21)$$

Correspondingly, the mode vectors \vec{n} are not all independent but restricted to belong to some fundamental domain, which can be determined as follows. The matrix (2.16) represents the \mathbf{Z}_N action on the mode vector \vec{n} for the torus wave functions. For $N \neq 2$, it amounts to a rotation with phase τ on the complex plane $u = -n_1 + \tau n_2$. This means that we can divide the space \mathbb{Z}^2 of all possible mode vectors \vec{n} into the origin, which is left fixed by Z_N , plus N sectors D_k , with $k = 0, \dots, N-1$, mapped into each other by Z_N . For $N > 2$, these domains can all be defined as $D_k = \{\vec{n} \in \mathbb{Z}^2 | (Z_N^k \vec{n})_1 < 0, (Z_N^k \vec{n})_2 \geq 0\}$, whereas for $N = 2$, they are given by $D_0 = \{\vec{n} \in \mathbb{Z}^2 | n_1 > 0 \oplus (n_1 = 0, n_2 > 0)\}$, $D_1 = \{\vec{n} \in \mathbb{Z}^2 | n_1 < 0 \oplus (n_1 = 0, n_2 < 0)\}$. The independent wave functions in (2.21) are then associated to $\vec{n} \in D_0$ and the origin, the ones associated to $\vec{n} \in D_k$ with $k \neq 0$ being the \mathbf{Z}_N -transformed of these.

It is now straightforward to characterize the spectrum of a generic T^2/\mathbf{Z}_N orbifold model. A field $\phi^g(z)$ with generic twisted boundary conditions

$$\phi^g(\tau z) = g \phi^g(z) \quad (2.22)$$

can be expanded in KK modes as

$$\phi^g(z) = \delta^{g,1} \phi_0^1 h_0^1(z) + \sum_{\vec{n} \in D_0} \phi_{\vec{n}}^g h_{\vec{n}}^g(z). \quad (2.23)$$

The mass $m_{\vec{n}}$ of the \vec{n} -mode is given by

$$m_{\vec{n}} = |\lambda_{\vec{n}}| = \frac{\sqrt{n_1^2 + n_2^2 - 2U_1 n_1 n_2}}{U_2 R}. \quad (2.24)$$

It is important to notice that the spectrum of modes does not depend on g , apart from the zero mode, which exists only if $g = 1$.

3. Higgs potential

The biggest problem in achieving gauge–Higgs unification in the minimal $5D$ case is the absence of a tree-level Higgs potential, resulting in too small a Higgs mass. This is the main reason for considering gauge–Higgs unification in $6D$, where such tree-level quartic term, arising from the gauge kinetic term, is naturally present. As suggested by several authors [4, 5], its presence can help getting realistic EWSB and Higgs masses. Most of the $6D$ models discussed so far, however, were based on \mathbf{Z}_2 orbifold constructions that necessarily lead to two charged Higgs doublets. In this case, the tree-level quartic term has a flat direction, just as in the MSSM, and therefore fluctuations along this direction only have radiatively induced masses, which in general tend to be too small.

We now focus our attention on T^2/\mathbf{Z}_N orbifold constructions with $N > 2$ leading to one Higgs doublet. As we shall show below, these models have a non-vanishing quartic tree-level potential, in contrast to the S^1/\mathbf{Z}_2 orbifold. This term is responsible for an important distinction between the interpretation of EWSB in T^2/\mathbf{Z}_N and S^1/\mathbf{Z}_2 orbifolds. In the $5D$ model, the vacuum expectation value (VEV) of the Higgs field is a flat direction of the classical potential and corresponds to a Wilson loop, which is also equivalent to a twist in the boundary conditions around S^1 [17]. In $6D$ models, on the contrary, the VEV of the Higgs field is *not* a flat direction of the classical potential, and such interpretation is missing. Indeed, there exist no continuous families of solutions to the usual orbifold consistency conditions for Wilson loops [18] in the case of $SU(3)$ gauge theories on T^2/\mathbf{Z}_N with $N > 2$. Only discrete Wilson loops are allowed. Nevertheless, the $5D$ and $6D$ models share the interesting property that the Higgs dynamics is much more constrained than what is just implied by the surviving gauge symmetry. This is a consequence of the non-linearly realized remnant of the higher-dimensional gauge symmetry associated to parameters depending on the internal coordinates, under which the Higgs field transforms inhomogeneously [19].

Let us now compute the classical Higgs potential that arises for the single Higgs models on T^2/\mathbf{Z}_N with $N = 3, 4, 6$. We choose $n_p = 1$, but the case $n_p = N - 1$ is perfectly similar up to an overall conjugation and therefore physically equivalent. The classical Lagrangian of the 6D theory is given simply by $L = -\frac{1}{2}\text{tr}F_{MN}^2$, where $F_{MN} = \partial_M A_N - \partial_N A_M - ig_6 [A_M, A_N]$. The Lagrangian for the zero modes A_μ^0 , A_z^0 and $A_{\bar{z}}^0$ is easily obtained by integrating over the internal torus. The result is given by

$$L = -\frac{1}{2}\text{tr}F_{\mu\nu}^{02} + 2\text{tr}|D_\mu A_z^0|^2 - g_4^2\text{tr}[A_z^0, A_{\bar{z}}^0]^2, \quad (3.1)$$

where $g_4 = g_6/\sqrt{V}$ is the gauge coupling of the 4D effective theory below the compactification scale, $F_{\mu\nu}^0 = \partial_\mu A_\nu^0 - \partial_\nu A_\mu^0 - ig_4[A_\mu^0, A_\nu^0]$ is the field strength of the massless 4D gauge bosons, and $D_\mu A_{z,\bar{z}}^0 = \partial_\mu A_{z,\bar{z}}^0 - ig_4[A_\mu^0, A_{z,\bar{z}}^0]$ is the covariant derivative on the Higgs field. The three weak gauge bosons and the hypercharge gauge boson are identified as $W_{\mu a} = A_{\mu a}^0$ for $a = 1, 2, 3$ and $B_\mu = A_{\mu 8}^0$. The zero modes of $A_\mu = \sum_a A_{\mu a} t^a$, where $a = 1, 2, 3, 8$, are then given by

$$A_\mu^0 = \frac{1}{2} \begin{pmatrix} W_\mu^3 + \frac{1}{\sqrt{3}} B_\mu & \sqrt{2} W_\mu^+ & 0 \\ \sqrt{2} W_\mu^- & -W_\mu^3 + \frac{1}{\sqrt{3}} B_\mu & 0 \\ 0 & 0 & -\frac{2}{\sqrt{3}} B_\mu \end{pmatrix}. \quad (3.2)$$

Similarly, the two complex components of the Higgs doublet are $h_u = A_{z+1}^0$ and $h_d = A_{z+2}^0$, and their complex conjugates are given by $h_u^* = A_{\bar{z}-1}^0$ and $h_d^* = A_{\bar{z}-2}^0$. The zero modes of $A_z = \sum_i A_{z+i} t^{+i}$ and $A_{\bar{z}} = \sum_i A_{\bar{z}-i} t^{-i}$ are thus given by

$$A_z^0 = \frac{1}{\sqrt{2}} \begin{pmatrix} 0 & 0 & h_u \\ 0 & 0 & h_d \\ 0 & 0 & 0 \end{pmatrix}, \quad A_{\bar{z}}^0 = \frac{1}{\sqrt{2}} \begin{pmatrix} 0 & 0 & 0 \\ 0 & 0 & 0 \\ h_u^* & h_d^* & 0 \end{pmatrix}. \quad (3.3)$$

Substituting these expressions in the Lagrangian, and switching from the $SU(3)$ to an $SU(2)$ notation, we finally find:

$$L = -\frac{1}{2}\text{tr}F_{\mu\nu}^{W2} - \frac{1}{4}F_{\mu\nu}^{B2} + \left| \left(\partial_\mu - ig_4 W_{\mu a} \frac{\tau_a}{2} - ig_4 \tan\theta_W \frac{1}{2} B_\mu \right) h \right|^2 - V_{\text{class}}(h), \quad (3.4)$$

where $\tan\theta_W = \sqrt{3}$ and

$$V_{\text{class}}(h) = \frac{g_4^2}{2} |h|^4. \quad (3.5)$$

The weak mixing angle arising in this construction is too large, but there are various ways of solving this problem, most notably by adding extra $U(1)$ gauge fields.

Quantum fluctuations induce a correction to the classical potential (3.5) and can trigger radiative symmetry breaking. The quantum effective potential can only depend on gauge-invariant quantities. These can be local or non-local in the compact

dimensions. Non-local operators involve Wilson lines wrapping around the internal space and are generated with finite coefficients whose size is controlled by the compactification scale $1/R$. The local and potentially divergent operators contributing to the Higgs potential arise from the non-derivative part of $F_{z\bar{z}}$, like the classical quartic term. Gauge invariance allows two possible classes of local operators of this kind: even powers of F_{MN} in the bulk or arbitrary powers of $F_{z\bar{z}}$ localized at the orbifold fixed points. In general, such terms will be generated at the quantum level with divergent coefficients. At one-loop order, the bulk operators that can lead to divergences in the Higgs potential are the gauge kinetic term F_{MN}^2 and a quartic coupling F_{MN}^4 , leading to quadratic and logarithmic divergences to $V(h)$ respectively. Localized operators are of the form $g_4^{2p} F_{z\bar{z}}^p$, where p is any positive integer. Quadratic and logarithmic divergences can arise from the tadpole operator $p = 1$ and the kinetic operator $p = 2$ respectively.

Since the quadratic bulk divergence gives rise only to a wave-function renormalization, we see that the only quadratic divergence to the Higgs potential comes from the localized tadpole operator $F_{z\bar{z}}$. In general, the latter induces a modification to the background and, in its non-abelian part, possible mixings between the Higgs and its KK modes, aside from a quadratically divergent mass term for the Higgs field h . In the rough approximation of neglecting the backreaction induced by the modified background and the KK mixings, effects that we will consider in section 5, and also neglecting all the logarithmic divergences, we see that the leading terms in the one-loop effective potential for the Higgs are

$$V_{\text{quant}}(h) = -\mu^2|h|^2 + \lambda|h|^4, \quad (3.6)$$

where μ^2 is a radiatively generated and possibly divergent mass term and $\lambda = g^2/2$ is the tree-level quartic term. Assuming $\mu^2 > 0$ so that EWSB can occur, we have $\langle|h|\rangle = v/\sqrt{2}$ with $v = \mu/\sqrt{\lambda}$. At the minimum,

$$\begin{aligned} m_H &= \sqrt{2}\mu = \sqrt{2}v\sqrt{\lambda} \\ m_W &= \frac{1}{2}gv. \end{aligned} \quad (3.7)$$

The ratio between m_H and m_W is therefore predicted in a completely model-independent way to be

$$\frac{m_H}{m_W} = \frac{2\sqrt{2}\lambda}{g} = 2. \quad (3.8)$$

Extra $U(1)$ fields, possibly needed to fix the weak-mixing angle to the correct value, do not modify eq. (3.8). The main radiative correction to eq. (3.8) arises from the Higgs wave-function distortion induced by the tadpole operator $F_{z\bar{z}}$, as explained in section 5. This effect can be estimated by Naïve Dimensional Analysis (NDA) to

give $O(1)$ corrections to eq. (3.8). In spite of this, the value of the Higgs mass is significantly increased with respect to the previously considered $5D$ models or \mathbf{Z}_2 orbifold constructions.

4. Divergent localized tadpole

We have seen that gauge invariance allows a localized interaction that is linear in the field strength, in addition to the universally allowed higher-order interactions involving even powers of the field strength. The localized interaction is particularly relevant, since it involves a mass term for the Higgs fields [11]. It has the form⁷

$$\mathcal{L}_{\text{tad}} = -i \sum_{k=1}^{\lfloor N/2 \rfloor} \frac{\mathcal{C}_k}{N_k} \sum_{i_k=1}^{N_k} \delta^{(2)}(z - z_{i_k}) F_{z\bar{z}}^8(z), \quad (4.1)$$

where \mathcal{C}_k are real coefficients of mass dimension 1 and $F_{z\bar{z}}^8$ is the field strength of the $U(1)$ component left unbroken by the orbifold breaking, which in terms of $6D$ fields reads

$$F_{z\bar{z}}^8 = \partial_z A_{\bar{z}}^8 - \partial_{\bar{z}} A_z^8 + g_6 f^{8bc} A_{zb} A_{\bar{z}c}. \quad (4.2)$$

In \mathbf{Z}_2 orbifold models, the parity symmetry $z \leftrightarrow \bar{z}$ can be implemented and it forbids the appearance of the operator (4.2), which is odd under this discrete symmetry [6, 11]. This parity can be generalized to \mathbf{Z}_N orbifolds, with $N > 2$, only if the twist matrix P is such that $P^2 = I$. The allowed form of the tadpole operator is then $\text{Im Tr } P F_{z\bar{z}}$, which automatically vanishes whenever $P^2 = I$. More precisely, we will see that the term associated to k in (4.1) can be written as $\text{Im Tr } P^k F_{z\bar{z}}$, implying that the tadpole vanishes in the sectors k such that $P^{2k} = I$, when the above \mathbf{Z}_2 symmetry can be implemented. Notice that projections that leave only one Higgs doublet do not satisfy $P^2 = I$ and hence are generally affected by tadpoles. We verify this statement by performing a detailed calculation of the coefficients \mathcal{C}_k for all \mathbf{Z}_N models at one-loop order. In particular we compute the contribution to the tadpole arising from gauge (and ghost) fields, and from an arbitrary bulk scalar or fermion in a representation \mathcal{R} of $SU(3)$. Possible localized boundary fields cannot minimally couple to the fields appearing in (4.2), because of the residual non-linearly realized gauge symmetries that are unbroken at the orbifold fixed points [19]. We therefore consider in the following $6D$ bulk fields only. This computation is also useful to understand whether and under what circumstances an accidental one-loop cancellation is possible.

⁷Abelian gauge fields that are present already before the orbifold projection and are unbroken can also develop a localized divergence term as in (4.1), but in this case the associated divergent mass term for even scalars, the last factor in (4.2), is absent.

The computation of Feynman diagrams on an orbifold can be nicely mapped to that on the corresponding covering torus by using a mode decomposition such that the effect of the orbifold projections amounts only to a non-conservation of the KK momentum in *non-diagonal* propagators,⁸ along the lines of [20]. Let us illustrate the formalism for a generic field $\Phi(z)$ on a T^2/\mathbf{Z}_N orbifold. The \mathbf{Z}_N group acts on Φ as described in (2.6), through the operator $\mathcal{P} = gR_s P_{\mathcal{R}}$, on both Lorentz and gauge indices: $\Phi(\tau z) = \mathcal{P}\Phi(z)$. We define the mode expansion of Φ as

$$\Phi(z) \equiv \sum_{\vec{n}} \Phi_{\vec{n}} f_{\vec{n}}(z), \quad (4.3)$$

where $f_{\vec{n}}$ is the basis of functions on T^2 defined in (2.17). The KK modes in (4.3), contrary to those appearing in (2.23), provide a redundant parametrization of Φ , since they are not all independent, owing to the condition (2.6). Their propagators will then be non-diagonal in the KK momentum space.

It is convenient to express Φ in terms of an unconstrained field $\tilde{\Phi}$ on T^2 with the same quantum numbers as Φ , so that (2.6) is automatically satisfied:

$$\Phi(z) = \frac{1}{N} \sum_{k=0}^{N-1} \mathcal{P}^k \tilde{\Phi}(\tau^{-k} z). \quad (4.4)$$

The propagator of Φ can then be written in terms of the propagator of $\tilde{\Phi}$ as⁹

$$\begin{aligned} \langle \Phi(z_1) \Phi^\dagger(z_2) \rangle &= \frac{1}{N^2} \sum_{k,l=0}^{N-1} \mathcal{P}^k \langle \tilde{\Phi}(\tau^{-k} z_1) \tilde{\Phi}^\dagger(\tau^{-l} z_2) \rangle (\mathcal{P}^\dagger)^l \\ &= \frac{1}{N} \sum_{k=0}^{N-1} \mathcal{P}^k \langle \tilde{\Phi}(\tau^{-k} z_1) \tilde{\Phi}^\dagger(z_2) \rangle, \end{aligned} \quad (4.5)$$

where the last simplification in the above expression is a consequence of the fact that the transformation $\tilde{\Phi}(z) \rightarrow \mathcal{P}^{-k} \tilde{\Phi}(\tau^k z)$ is by assumption a symmetry of the action. The propagator of $\tilde{\Phi}$ is the standard propagator on the torus and can be written as

$$\langle \tilde{\Phi}(z_1) \tilde{\Phi}^\dagger(z_2) \rangle \equiv \sum_{\vec{n}} \tilde{G}_{\vec{n}} f_{\vec{n}}(z_1 - z_2),$$

where $\tilde{G}_{\vec{n}}$ denotes the standard form of the propagator in momentum space, and the torus periodicity conditions result only in the quantization of the KK momenta in the

⁸An alternative procedure to compute Feynman diagrams on orbifolds is obtained by directly considering physical modes only, as derived in section 2. In this case, the propagators for all fields are diagonal in the KK momenta and the momentum non-conservation arises from the interaction vertices. As a further consistency check of our results, we have also computed both the 1- and 2-point functions in this way and found perfect agreement between the two methods.

⁹We write the propagator in the form of a correlator among Φ and its hermitian conjugate Φ^\dagger , but our formalism clearly applies to real fields as well.

$$\begin{array}{c}
\vec{n} \\
\longrightarrow \\
B
\end{array}
\longrightarrow
\begin{array}{c}
\textcircled{k} \\
\longrightarrow \\
A
\end{array}
\begin{array}{c}
Z_N^{-k} \vec{n} \\
\longrightarrow \\
A
\end{array}
= \frac{1}{N} \left[\mathcal{P}^k \cdot \tilde{G}_{\vec{n}} \right]_{AB}$$

Figure 2: Feynman rule for the propagators on an orbifold. In the figure, A, B are a generic set of indices labelling the state and $k = 0, \dots, N - 1$ is the possible twist of the propagator.

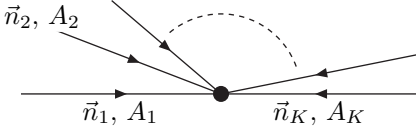
$$V = \mathcal{V}_{\{A_1, \vec{n}_1\}, \dots, \{A_K, \vec{n}_K\}} \Phi_{\{A_1, \vec{n}_1\}} \dots \Phi_{\{A_K, \vec{n}_K\}} \sim$$


Figure 3: The diagrammatic representation of a generic effective vertex V .

internal directions. Recalling that the orbifold action on the KK momenta is given by (2.19), we then find

$$\langle \Phi(z_1) \Phi^\dagger(z_2) \rangle = \frac{1}{N} \sum_{k=0}^{N-1} \sum_{\vec{n}} \mathcal{P}^k \tilde{G}_{\vec{n}} f_{Z_N^{-k} \vec{n}}(z_1) f_{\vec{n}}^\dagger(z_2), \quad (4.6)$$

whose Fourier transform is

$$\langle \Phi_{\vec{m}} \Phi_{\vec{n}}^\dagger \rangle = \frac{1}{N} \sum_{k=0}^{N-1} \mathcal{P}^k \tilde{G}_{\vec{n}} \delta_{\vec{m}, Z_N^{-k} \vec{n}}. \quad (4.7)$$

Equation (4.7) shows that the propagator on an orbifold can be written as the sum of N propagators, of which all but the first violate momentum conservation. Any internal line of a Feynman diagram is then the sum of the “ k ” propagators shown in Fig. 2, in which an incoming momentum \vec{n} is changed into an outgoing one $Z_N^{-k} \vec{n}$. When using the Feynman rule shown in Fig. 2, an orientation of the propagator is needed so as to distinguish incoming and outgoing lines. If the field is complex this orientation is naturally provided; if it is real, one orientation has to be chosen to apply the rule of Fig. 2, but clearly the result does not depend on this choice.

In this approach, all the interaction vertices conserve the KK momenta and any diagram can thus be computed by simply applying the usual Feynman rules, inserting the orbifold propagator as shown in Fig. 2. The computation is, however, simplified by noting that any interaction vertex has to be \mathbf{Z}_N -invariant. Its action on a set of K fields, with modes $\Phi_{\vec{n}_f}$ ($f = 1, \dots, K$), is $\Phi_{\vec{n}_f} \rightarrow \mathcal{P}_f^k \Phi_{Z_N^{-k} \vec{n}_f}$. This leads to the following relation, valid for any interaction vertex \mathcal{V} (see Fig. 3):

$$\mathcal{V}_{\{B_1, Z_N^{-k} \vec{n}_1\}, \dots, \{B_K, Z_N^{-k} \vec{n}_K\}} \left[\mathcal{P}_1^k \right]_{B_1 A_1} \dots \left[\mathcal{P}_K^k \right]_{B_K A_K} = \mathcal{V}_{\{A_1, \vec{n}_1\}, \dots, \{A_K, \vec{n}_K\}}, \quad (4.8)$$

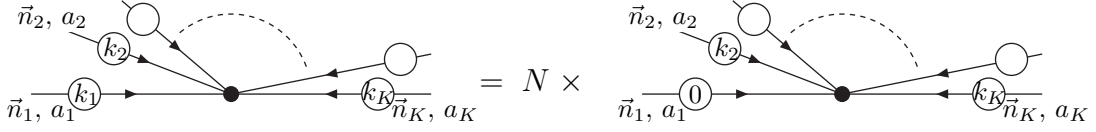


Figure 4: Equivalence between interaction vertices on a \mathbf{Z}_N orbifold.

where A_f, B_f represent both Lorentz and gauge indices of the various fields. Thanks to (4.8), we notice that (see Fig. 4) if K propagators are attached to a vertex, we do not have to sum over all their K independent twists, as one of them can be set to zero, simply giving an extra factor of N . Notice that there is no need for the vertex V to be elementary, *i.e.* to appear in the tree-level action. This general result turns out to be useful in computing the Higgs 2-point function. In this case it also holds for on-shell external lines, because $\vec{n} = \vec{0}$ is a fixed point of Z_N , and \mathcal{P} acts as the identity on the physical $\vec{0}$ modes.

We extract the coefficients \mathcal{C}_k by computing the 1-point function of all the KK modes of A_z^8 . We then work out also the 2-point function for the zero-mode h of the Higgs field, defined as in (3.3), to extract its finite non-local mass terms and to check the 1-point function computation. In order to find an expression that can be directly compared with the computation of 1- and 2-point functions for KK modes, we need to work out more explicitly eq. (4.1). Using the mode expansion (4.3), we easily find:

$$\int dz^2 \mathcal{L}_{\text{tad}} = - \sum_{k=1}^{[N/2]} \mathcal{C}_k \left[\sum_{\vec{n}} \frac{1}{N_k} \sum_{i_k=1}^{N_k} f_{\vec{n}}(z_{i_k}) (p_{z,\vec{n}} A_{\bar{z},\vec{n}}^8 - p_{\bar{z},\vec{n}} A_{z,\vec{n}}^8) + \frac{g_4}{\sqrt{V}} (i f^{8+i-j}) h_i h_j^\dagger \right] + \dots, \quad (4.9)$$

where $p_{z,\vec{m}} = \frac{i}{\sqrt{2}} \lambda_{\vec{m}}$, $p_{\bar{z},\vec{m}} = -\frac{i}{\sqrt{2}} \bar{\lambda}_{\vec{m}}$ are the internal KK momenta, with $\lambda_{\vec{m}}, \bar{\lambda}_{\vec{m}}$ as in (2.18), and the dots stand for all the remaining quadratic couplings between all the KK excitations of $A_{z,+i}$ and $A_{\bar{z},-j}$. Using the identity

$$\frac{1}{N_k} \sum_{i_k=1}^{N_k} f_{\vec{n}}(z_{i_k}) = \frac{1}{\sqrt{V}} \delta_{(1-Z_N^k)^{-1} \vec{n} \in \mathbf{Z}^2}, \quad (4.10)$$

valid for all the T^2/\mathbf{Z}_N orbifolds, the contributions of the two terms in (4.9) to the 1- and 2-point functions are found to be

$$\langle A_{z,\vec{n}}^8 \rangle = i p_{\bar{z},\vec{n}} \sum_{k=1}^{[N/2]} \frac{\mathcal{C}_k}{\sqrt{V}} \delta_{(1-Z_N^k)^{-1} \vec{n} \in \mathbf{Z}^2}, \quad (4.11)$$

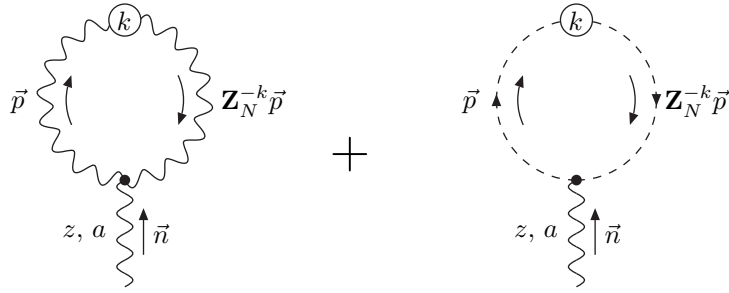


Figure 5: The gauge and ghost contributions to the 1-point function $\langle A_{z,\vec{n}}^a \rangle$.

$$\langle h_i h_j^\dagger \rangle = g_4 f^{8+i-j} \sum_{k=1}^{[N/2]} \frac{\mathcal{C}_k}{\sqrt{V}}. \quad (4.12)$$

Notice that the Higgs mass term arising from (4.12) is sensible only to the sum of the tadpole coefficients \mathcal{C}_k .

4.1. 1-point function

According to the considerations made at the beginning of this section, all the Feynman rules for the vertices are the standard ones, whereas the propagator has to be replaced (see Fig. 5) by its twisted version, as in Fig. 2. In the following we adopt the Feynman gauge, obtained through the choice $\xi = 1$ in the general gauge-fixing term

$$\mathcal{L}_{\text{gf}} = -\frac{1}{2\xi} \sum_{a=1}^8 \left[\partial_\mu A^{\mu,a} - \xi (\partial_z A_{\bar{z}}^a + \partial_{\bar{z}} A_z^a) \right]^2. \quad (4.13)$$

By 4D Lorentz invariance, a tadpole can be generated only for the field components A_z^a and $A_{\bar{z}}^a$. An explicit computation of this tadpole shows that it has the form:

$$\langle A_{z,\vec{n}}^a \rangle = g_4 \sum_{k=0}^{N-1} \hat{\xi}_k^a \sum_{\vec{m}} \int \frac{d^4 p}{(2\pi)^4} \frac{p_{\bar{z},\vec{m}}}{p^2 - 2|p_{z,\vec{m}}|^2} \delta_{\vec{n},(1-Z_N^{-k})\vec{m}}, \quad (4.14)$$

where $\hat{\xi}_k^a$ are numerical coefficients depending on the kind of field running in the loop and $p^2 = p_\mu p^\mu$ is the 4D momentum squared. The sector $k = 0$ never contributes. For the sectors $k \neq 0$, the δ -function in KK space relates the internal momenta of the virtual state to that of the external particle: $p_{\bar{z},\vec{m}} = (1 - \tau^k)^{-1} p_{\bar{z},\vec{n}}$. We can then perform the sum over m , and we are left with the condition $(1 - Z_N^{-k})^{-1} \vec{n} \in \mathbb{Z}^2$. Therefore, the quadratically divergent part of eq. (4.14) has the form of eq. (4.11). This condition can easily be shown to be equivalent to $(1 - Z_N^{k-N})^{-1} \vec{n} \in \mathbb{Z}^2$, so that in eq. (4.14) the sector $N - k$ contributes just as the sector k . The two contributions of these conjugate sectors can be paired, as expected, and simply yield twice the

real part of one of them (with the obvious exception of the sector $k = N/2$ that, if present, must be counted only once). Finally, defining the new coefficients $\xi_k^a = -2^{1-\delta_{k,N/2}}\tau^{-k/2}N_k^{-1/2}\hat{\xi}_k^a$, eq. (4.14) can be rewritten in the more suggestive form

$$\langle A_{z,\bar{n}}^a \rangle = -g_4 D(\Lambda) \sum_{k=1}^{[N/2]} p_{z,\bar{n}} \delta_{(1-Z_N^k)^{-1}\bar{n} \in \mathbf{Z}^2} \text{Im} \xi_k^a + \dots, \quad (4.15)$$

where

$$D(\Lambda) = i \int \frac{d^4 p}{(2\pi)^4} \frac{1}{p^2} = \frac{1}{16\pi^2} \Lambda^2. \quad (4.16)$$

The dots in (4.15) stand for additional logarithmically divergent and finite subleading corrections. These corrections are very similar to those found in [21] for the FI term in 5D SUSY theories on $S^1/(\mathbf{Z}_2 \times \mathbf{Z}'_2)$, and are associated to interactions involving additional internal derivatives $\partial_z \partial_{\bar{z}}$ acting on $F_{z\bar{z}}^8$. Notice also that in the presence of an additional bulk mass term M for the fields running in the loop, which is possible for instance for scalar fields, eq. (4.16) gets modified through the simple substitution $\Lambda^2 \rightarrow \Lambda^2 - 2M^2 \ln(\Lambda/M)$.

The contributions to ξ_a^k of the gauge and ghost fields in the adjoint representation, and of complex scalar or Weyl spinor fields in an arbitrary representation \mathcal{R} and with overall twist g , are found to be:

$$(\xi_k^a)_{\text{gauge}} = \frac{-1}{NN_k^{1/2}} \left[5(\tau^{\frac{k}{2}} + \tau^{-\frac{k}{2}}) - (\tau^{\frac{3k}{2}} + \tau^{-\frac{3k}{2}}) \right] \text{Tr}_{\text{adj}} [P^k t^a], \quad (4.17)$$

$$(\xi_k^a)_{\text{scalar}} = \frac{-2}{NN_k^{1/2}} g^k (\tau^{\frac{k}{2}} + \tau^{-\frac{k}{2}}) \text{Tr}_{\mathcal{R}} [P^k t^a], \quad (4.18)$$

$$(\xi_k^a)_{\text{fermion}} = (4) \frac{2^{1-\delta_{k,N/2}}}{NN_k^{1/2}} (g\tau^{\frac{1}{2}})^k \text{Tr}_{\mathcal{R}} [P^k t^a], \quad (4.19)$$

where $(\xi_k^a)_{\text{gauge}}$ also contains the ghost contribution. The gauge trace appearing in the above coefficients is as expected to differ from zero only for $a = 8$, reflecting the fact that only a $U(1)$ tadpole is allowed by the gauge symmetry. It is easily evaluated by recalling the definition of the twist matrix $P_{\mathcal{R}}$, eq. (2.7), and exploiting the decomposition of the representation \mathcal{R} under $SU(3) \rightarrow SU(2) \times U(1)$. Denoting by $d_{\mathcal{R}_r}$ and $q_{\mathcal{R}_r}$ the dimensionality and the charge under $Q_{\mathcal{R}} = \frac{1}{\sqrt{3}}t_{\mathcal{R}}^8$ of the r -th component \mathcal{R}_r in the decomposition $\mathcal{R} \rightarrow \oplus_r \mathcal{R}_r$, we find:

$$\text{Tr}_{\mathcal{R}} [P^k t^8] = \sqrt{3} \sum_{\mathcal{R}_r} d_{\mathcal{R}_r} q_{\mathcal{R}_r} \tau^{2n_p(\frac{n_{\mathcal{R}}}{3} + q_{\mathcal{R}_r})k}. \quad (4.20)$$

Notice that the gauge contribution to the tadpole vanishes at 1-loop order for the \mathbf{Z}_2 case. The same happens for any scalar or fermion contribution in a real representation.

This can be seen by using the relation (valid for any \mathbf{Z}_N orbifold):¹⁰

$$\mathrm{Tr}_{\mathcal{R}} [P^k t^8] = -\mathrm{Tr}_{\mathcal{R}} [P^{-k} t^8] , \quad \text{if } \mathcal{R} \text{ real.} \quad (4.21)$$

This result is in agreement with that found in [11], where it was also generalized to the 2-loop case. On the contrary, for $N = 3, 4, 6$, there is always some tadpole coefficient that is non-vanishing for the single-Higgs projections. The tadpole can only vanish for the zero-Higgs cases $N = 4, n_p = 2$ and $N = 6, n_p = 3$, since they correspond to vanishing $\mathrm{Im} \mathrm{Tr}_{\mathrm{adj}} [P^k t^a]$.

The fermion contribution (4.19) has a structure that resembles that of the $4D$ mixed $U(1)$ -gravitational anomaly induced at the fixed points by $6D$ Weyl fermions. The structure of this anomaly can be understood using Fujikawa's approach to anomalies, as was done in [22] for string-derived orbifold models. The total contribution to localized mixed $U(1)$ -gravitational anomalies from a $6D$ fermion is proportional to $\sum_{k=1}^{\lfloor N/2 \rfloor} N_k \mathrm{Im} (\xi_k^8)_{\mathrm{fermion}}$. This expression can be written as a projector over massless $4D$ fermions, weighted by their $4D$ chirality, and is thus proportional to the sum over $U(1)$ charges of the $4D$ chiral fermions. Notice, however, that $6D$ fermions always contribute to the tadpole with the same sign, independently of their $6D$ chirality, as already noted for the \mathbf{Z}_2 case in [11]. Since a flip of the $6D$ chirality amounts to a flip of the $4D$ one, this implies that the sum over all possible fermion contributions to the tadpole does not coincide with the total mixed $U(1)$ -gravitational anomaly of the $4D$ fermion spectrum, even when the factor N_k can be factorized out of the trace, as in the \mathbf{Z}_2 and \mathbf{Z}_3 models. This means that even when the scalar and gauge contribution to the tadpole vanish, the requirements of vanishing integrated tadpole and $U(1)$ -gravitational anomaly cancellation are in general independent constraints.

In order to relate the coefficients ξ_k^8 to the coefficients \mathcal{C}_k appearing in (4.1), we must compare eq. (4.15) with eq. (4.11), which have as expected the same structure. The result is

$$\mathcal{C}_k = g_4 \sqrt{V} D(\Lambda) \mathrm{Im} \xi_k^8 . \quad (4.22)$$

We summarize in Table 2 the contribution of a Weyl fermion to \mathcal{C}_k for all possible twists and for the first few $SU(3)$ representations. Notice that the contribution of a fermion with twist g in the conjugate representation $\bar{\mathcal{R}}$ is equal to that of a fermion twisted by $\bar{g}\bar{\tau}$ in the representation \mathcal{R} . Similarly, a scalar in the $\bar{\mathcal{R}}$ with twist g contributes as one in the \mathcal{R} with conjugate twist \bar{g} . The sum over all possible twists for any scalar or fermion contribution always vanishes, since in this case one reconstructs the matter content that would appear on the covering torus, which cannot give rise to any localized divergence. We see that for $N = 3, 4, 6$ and for any choice of fermion

¹⁰Actually the scalar contribution in the \mathbf{Z}_2 model vanishes for any representation, not only for real ones.

representations, it is impossible to cancel the total (gauge+ghost+fermion) one-loop contribution to each tadpole coefficient¹¹, although one can obtain their global cancellation, namely the cancellation of their integral over the compact space $\sum_k \mathcal{C}_k = 0$. This seems to be possible, without scalars, only for \mathbf{Z}_4 with an odd number of $6D$ Weyl fermions in suitable representations. If one includes scalars, an accidental local one-loop cancellation of the tadpole is possible, but in this case one needs a symmetry to protect the mass M of the $6D$ scalars, which is otherwise expected to be at the cut-off scale Λ , and reintroduce a quadratic sensitivity to the latter.

\mathbf{Z}_2	1	τ
$c_1(\mathbf{3})$	-4	4
$c_1(\mathbf{6})$	4	-4
$c_1(\mathbf{8})$	0	0
$c_1(\mathbf{10})$	-12	12

\mathbf{Z}_3	1	τ	τ^2
$c_1(\mathbf{3})$	-4	-4	8
$c_1(\mathbf{6})$	-20	16	4
$c_1(\mathbf{8})$	12	-24	12
$c_1(\mathbf{10})$	12	12	-24

\mathbf{Z}_4	1	τ	τ^2	τ^3
$c_1(\mathbf{3})$	0	-8	0	8
$c_1(\mathbf{6})$	-24	-16	24	16
$c_1(\mathbf{8})$	24	-24	-24	24
$c_1(\mathbf{10})$	-48	24	48	-24
$c_2(\mathbf{3})$	-4	4	-4	4
$c_2(\mathbf{6})$	4	-4	4	-4
$c_2(\mathbf{8})$	0	0	0	0
$c_2(\mathbf{10})$	-12	12	-12	12

\mathbf{Z}_6	1	τ	τ^2	τ^3	τ^4	τ^5
$c_1(\mathbf{3})$	4	-4	-8	-4	4	8
$c_1(\mathbf{6})$	-4	-32	-28	4	32	28
$c_1(\mathbf{8})$	36	0	-36	-36	0	36
$c_1(\mathbf{10})$	-60	-84	-24	60	84	24
$c_2(\mathbf{3})$	-4	-4	8	-4	-4	8
$c_2(\mathbf{6})$	-20	16	4	-20	16	4
$c_2(\mathbf{8})$	12	-24	12	12	-24	12
$c_2(\mathbf{10})$	12	12	-24	12	12	-24
$c_3(\mathbf{3})$	-4	4	-4	4	-4	4
$c_3(\mathbf{6})$	4	-4	4	-4	4	-4
$c_3(\mathbf{8})$	0	0	0	0	0	0
$c_3(\mathbf{10})$	-12	12	-12	12	-12	12

Table 2: The contribution to the tadpole coefficients \mathcal{C}_k from Weyl fermions for various representations and all choices of the phase g . We report the quantity $c_k = \sqrt{3} N \text{Im}[\xi_k^g]$, which for the gauge contribution is given by $c_1 = 0$ for \mathbf{Z}_2 , $c_1 = -21$ for \mathbf{Z}_3 , $c_1 = -36$ and $c_2 = 0$ for \mathbf{Z}_4 , and $c_1 = -45$, $c_2 = -21$ and $c_3 = 0$ for \mathbf{Z}_6 . In all cases, we are considering the projection with $n_p = 1$, giving single-Higgs models for $N \neq 2$.

4.2. 2-point function

We now compute the one-loop 2-point function for the Higgs field, at zero external $4D$ and KK momentum. Contrarily to the 1-point function, which we have computed

¹¹Our result for the gauge+ghost one-loop contribution to the tadpole in the \mathbf{Z}_4 model is in disagreement with the result of [6], where it was found to vanish.

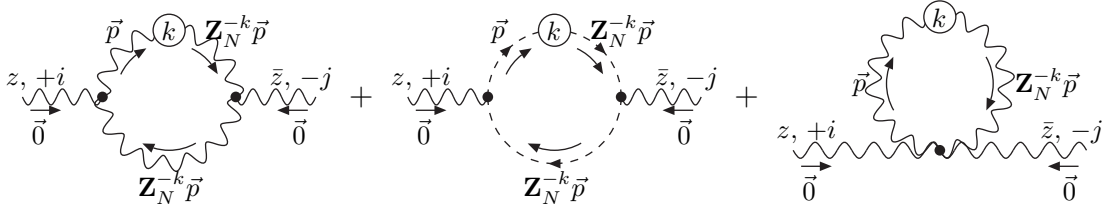


Figure 6: The gauge and ghost contributions to the 2-point function $\langle h_i h_j^\dagger \rangle$.

for any external KK momentum, this correlation gives us information only on the form of the operator (4.1) integrated over the compact space (see eq. (4.12)). Nevertheless, it provides an important independent check of the 1-point function computation and also allows the extraction of the finite non-local contributions to the Higgs mass.

Thanks to the property displayed in Fig. 4, each of the diagrams contributing to the one-loop Higgs mass contains only one twisted propagator with twist k . The diagrams with $k = 0$ give a finite contribution, which reproduces up to a $1/N$ factor the result that would be obtained for a theory on the covering torus T^2 . The remaining contributions arising from the diagrams with the insertion of a propagator with $k \neq 0$ are instead divergent. Owing to momentum conservation at the vertices, the internal KK momentum in the twisted internal lines has to vanish (see Fig. 6). The general structure of the Higgs 2-point function is then given by:¹²

$$\langle h_i h_j^\dagger \rangle = g_4^2 f_8^{+i-j} \xi_{\text{div}}^8 D(\Lambda) + ig_4^2 \delta_{ij} \xi_{\text{fin}}^8 F(R), \quad (4.23)$$

with $D(\Lambda)$ as in (4.16) and

$$F(R) = i \int \frac{d^4 p_4}{(2\pi)^4} \sum_{\vec{n} \in \mathbf{Z}^2} \frac{p^2}{(p^2 - 2|p_{z,\vec{n}}|^2)^2} = \frac{U_2}{4\pi^5 R^2} \sum_{\vec{n} \neq \vec{0}} |n_1 + U n_2|^{-4}. \quad (4.24)$$

It is straightforward to compute the diagrams controlling the divergent part. Note that ghosts do not contribute, because their coupling to the Higgs is proportional to the KK momentum. Thanks to the identities

$$\begin{aligned} \text{Tr}_{\mathcal{R}} [t^{+i} t^{-j} P^k] &= \tau^l \text{Tr}_{\mathcal{R}} [t^{-j} t^{+i} P^k], \\ \text{Tr}_{\mathcal{R}} [t^{-j} t^{+i} P^k] &= -i f_8^{+i-j} \frac{1}{1 - \tau^l} \text{Tr}_{\mathcal{R}} [t^8 P^k], \end{aligned} \quad (4.25)$$

the result can be rewritten as

$$\xi_{\text{div}}^8 = \sum_{k=1}^{[N/2]} \text{Im} \xi_k^8, \quad (4.26)$$

¹²Equation (4.23) is valid also for the \mathbf{Z}_2 model, where two Higgs fields are present. In this case, there are additional 2-point correlators that we neglect. See *e.g.* [5].

where the ξ_k^8 's turn out to precisely match the expressions (4.17)–(4.19) extracted from the 1-point function computation. This result represents a non-trivial check of that computation. Indeed, comparing eq. (4.23) with eq. (4.12), we deduce that

$$\sum_{k=1}^{[N/2]} \mathcal{C}_k = g_4 \sqrt{V} D(\Lambda) \xi_{\text{div}}^8 \quad (4.27)$$

which is compatible with the result in eq. (4.22) thanks to the relation (4.26).

The diagrams contributing to the finite part can be computed as well, and the coefficients of the finite part are found to be given by:

$$(\xi_{\text{fin}}^8)_{\text{gauge}} = 2 \frac{4}{N} C(\text{Adj}), \quad (4.28)$$

$$(\xi_{\text{fin}}^8)_{\text{scalar}} = \frac{4}{N} C(\mathcal{R}), \quad (4.29)$$

$$(\xi_{\text{fin}}^8)_{\text{fermion}} = -2 \frac{4}{N} C(\mathcal{R}), \quad (4.30)$$

in terms of the quadratic Casimir $C(\mathcal{R})$ of the representation \mathcal{R} , defined by the relation $\text{Tr}_{\mathcal{R}} [t^a t^b] = C(\mathcal{R}) \delta^{ab}$, so that $C(\text{Fund}) = \frac{1}{2}$ and $C(\text{Adj}) = 3$.

5. Phenomenological implications

In sections 3 and 4 we have shown how $6D$ gauge theories on orbifold models can lead to a beautiful prediction for the Higgs mass, but at the same time they are affected by a quadratic divergence arising from a localized tadpole term. It is thus natural to try to understand whether and to what extent such models can be considered for realistic model building.

One of the main generic problems in models with gauge–Higgs unification is how to accommodate the standard matter fields. A possibility is to introduce them at the fixed points of the orbifold. Standard Yukawa couplings cannot be directly introduced, because they would violate the higher-dimensional symmetry. However, effective non-local Yukawa couplings can be generated by introducing mixings between the matter fields and additional heavy fermions in the bulk, which are then integrated out [6, 7]. In this situation, the localized matter field will in general influence the one-loop tadpole (4.2), but since this requires mixing insertions, only logarithmic divergences can be induced. The weak mixing angle, whose value in the basic $SU(3)$ model is too large, can be fixed by introducing additional $U(1)$ gauge fields in the bulk (see *e.g.* [5, 7]), as mentioned in section 2.

The real issue is that the presence of the quadratically divergent term (4.1) can destabilize the electroweak scale. It must therefore be understood how much (if any) progress has been achieved with respect to the SM, as far as the little hierarchy

problem is concerned. The abelian and non-abelian components of the localized operator (4.1) induce respectively a non-trivial background for the field A_z^8 and a mass term for the Higgs doublet A_z^{-i} . The latter can generate not only a mass term for the 4D Higgs field, but also mixings between all its KK partners. These mixings can be neglected only if their magnitude is much smaller than $1/R$, the typical mass of KK modes. In our case, $\mathcal{C}_k > 1/R$ (see below) and the effect of all these mixings, as well as that of the non-trivial background for A_z^8 , must be taken into account. In order to see if and how much the EWSB scale is sensitive to this divergence, one has to compute the background value of A_z^8 and study the quantum fluctuations around it, to get the physical masses of the various fields, in particular for A_z^{-i} . Luckily, a similar analysis has already been performed in [15], where the effect of localized FI terms in 6D orbifold models has been studied (see also [23, 24]). As already mentioned, the tadpole (4.1) can be interpreted as a FI term in SUSY theories; this suggests a correspondence that allows a study of its physical consequences even in our non-SUSY set-up. The background induced by the tadpole can be explicitly found as follows. If one sets to zero all 4D gauge fields, the effective potential one obtains for the scalar fields A_z^a , in the unitary gauge $\xi \rightarrow \infty$ in (4.13), can be written, up to some irrelevant constant terms, as

$$V = \frac{1}{2} \sum_{a=1}^3 |F_{z\bar{z}}^a|^2 + |F_{z\bar{z}}^{-i}|^2 + \frac{1}{2} |F_{z\bar{z}}^8 - i \sum_{k=1}^{[N/2]} \frac{\mathcal{C}_k}{N_k} \sum_{i_k=1}^{N_k} \delta^{(2)}(z - z_{i_k})|^2. \quad (5.1)$$

The potential (5.1) is a sum of squares and thus, as happens for the D -term potential of SUSY theories, configurations where it vanishes are automatically consistent classical backgrounds. In the particular case where the tadpole globally vanishes, that is $\sum_k \mathcal{C}_k = 0$, the background value of the fields can be determined by proceeding as in [15]. The result is that $\langle A_z^8 \rangle = i \partial_z W$, where the function W is a linear combination of scalar Green functions on the internal T^2 . The existence of a zero-mode solution $A_{z,0}^{-i}$ for the field A_z^{-i} in the presence of this background is ensured by the existence of a solution to the first-order equation

$$F_{z\bar{z}}^{-i} = \left(\partial_{\bar{z}} + i g_6 \tan \theta_W \frac{1}{2} \langle A_z^8 \rangle \right) A_{z,0}^{-i} = 0. \quad (5.2)$$

We refer the reader to [15] for a detailed analysis of the profile of the zero mode wave function in the internal space. The above reasoning shows that a globally vanishing tadpole does not give rise to any quadratic divergence in the Higgs mass parameter μ^2 appearing in (3.6). In other words, a globally vanishing tadpole is harmless for EWSB, which is governed by the finite non-local contributions to the 2-point function, proportional to (4.24), which for simplicity we have neglected in these simple lines of arguments. In the presence of globally vanishing one-loop tadpole, the little hierarchy

problem is then solved. The non-trivial profile for the Higgs field, however, induces large corrections to (3.8), since this ratio depends on the integral of the Higgs profile in the internal directions. As mentioned in section 3, such corrections are estimated to be of $O(1)$ and thus might significantly alter the tree-level result (3.8).

To be more quantitative, we can rely on the higher-dimensional generalization of the NDA [25]. We denote in short by $l_4 = 16\pi^2$ and $l_6 = 128\pi^3$ the $4D$ and $6D$ loop factors. The relation between the cut-off scale Λ and the compactification scale $1/R$ is then estimated to be $\Lambda \sim g_4^{-1}(2\pi R)^{-1}\sqrt{l_6}$, which for the EW coupling yields $\Lambda \sim 10/R$. In this way we obtain an estimate for the tadpole coefficient \mathcal{C}_k that is in agreement with the direct one-loop result reported in (4.22) and of order $l_6/(2\pi R g_4 l_4) > 1/R$, as mentioned. On the other hand, the value of μ^2 in eq. (3.6) induced by finite non-local corrections is of order $\mu^2 \sim g_4^2/(l_4 R^2)$, and from (3.7) one estimates $1/R \sim 1$ TeV and $\Lambda \sim 10$ TeV, which are compatible with present experimental bounds in a natural way. On the other hand, for a globally non-vanishing tadpole, it is reasonable to expect to have effectively $\mu^2 \sim g_4^2 \Lambda^2/l_4$. From (3.7) one now estimates $\Lambda \sim 1$ TeV, corresponding to $1/R \sim 100$ GeV. The amount of fine-tuning that is needed in this case is about the same as in the SM, and there is no progress concerning the little hierarchy problem.

Summarizing, we have shown that there exists a class of $6D$ \mathbf{Z}_N orbifold models with gauge–Higgs unification that lead to a single Higgs doublet with the tree-level prediction $m_H = 2m_W$, and for which the EWSB scale is sufficiently stable, provided that the one-loop integrated tadpole vanishes. Although we have not provided in this paper a complete and realistic $6D$ model with gauge–Higgs unification, which would require in particular to find an anomaly-free fermion spectrum with a globally vanishing tadpole, we think that it will be very interesting to analyse the phenomenological aspects of the single Higgs T^2/\mathbf{Z}_N models discussed in this paper.

Acknowledgments

We would like to thank S. Bertolini, R. Contino, A. Pomarol, M. Quiros, R. Rattazzi, A. Romanino and A. Schwimmer for many fruitful discussions. This research work was partly supported by the European Community through a Marie Curie fellowship and the RTN network contracts HPRN-CT-2000-00131 and HPRN-CT-2000-00148. M.S., L.S. and A.W. acknowledge CERN, and M.S. and A.W. acknowledge Rome University “La Sapienza”, where part of this work was done.

References

- [1] R. Barbieri, A. Strumia, Phys. Lett. B **462** (1999) 144 [hep-ph/9905281].
- [2] N. S. Manton, Nucl. Phys. B **158** (1979) 141; D. B. Fairlie, Phys. Lett. B **82** (1979)

- 97; J. Phys. G **5** (1979) L55; P. Forgacs, N. S. Manton, Commun. Math. Phys. **72** (1980) 15; G. Chapline, R. Slansky, Nucl. Phys. B **209** (1982) 461; S. Randjbar-Daemi, A. Salam, J. Strathdee, Nucl. Phys. B **214** (1983) 491; N. V. Krasnikov, Phys. Lett. B **273** (1991) 246.
- [3] H. Hatanaka, T. Inami, C. Lim, Mod. Phys. Lett. A **13** (1998) 2601 [hep-th/9805067]; G. R. Dvali, S. Randjbar-Daemi, R. Tabbash, Phys. Rev. D **65** (2002) 064021 [hep-ph/0102307].
- [4] N. Arkani-Hamed, A. G. Cohen, H. Georgi, Phys. Lett. B **513** (2001) 232 [hep-ph/0105239].
- [5] I. Antoniadis, K. Benakli, M. Quiros, New J. Phys. **3** (2001) 20 [hep-th/0108005].
- [6] C. Csaki, C. Grojean, H. Murayama, Phys. Rev. D **67** (2003) 085012 [hep-ph/0210133].
- [7] C. A. Scrucca, M. Serone, L. Silvestrini, Nucl. Phys. B **669** (2003) 128 [hep-ph/0304220].
- [8] L. J. Hall, Y. Nomura, D. R. Smith, Nucl. Phys. B **639** (2002) 307 [hep-ph/0107331]; G. Burdman, Y. Nomura, Nucl. Phys. B **656** (2003) 3 [hep-ph/0210257]; N. Haba, Y. Shimizu, Phys. Rev. D **67** (2003) 095001 [hep-ph/0212166]; K. Choi *et al.*, hep-ph/0312178; I. Gogoladze, Y. Mimura, S. Nandi, Phys. Lett. B **560** (2003) 204 [hep-ph/0301014]; *ibid.* **562** (2003) 307 [hep-ph/0302176]; hep-ph/0311127.
- [9] I. Antoniadis, K. Benakli, Phys. Lett. B **326** (1994) 69 [hep-th/9310151].
- [10] C. Biggio, F. Feruglio, I. Masina, M. Perez-Victoria, Nucl. Phys. B **677** (2004) 451 [hep-ph/0305129].
- [11] G. von Gersdorff, N. Irges, M. Quiros, Phys. Lett. B **551** (2003) 351 [hep-ph/0210134].
- [12] N. Arkani-Hamed, T. Gregoire, J. Wacker, JHEP **0203** (2002) 055 [hep-th/0101233].
- [13] R. Sekhar Chivukula, D. A. Dicus, H. J. He, Phys. Lett. B **525** (2002) 175 [hep-ph/0111016]; R. S. Chivukula, H. J. He, Phys. Lett. B **532** (2002) 121 [hep-ph/0201164]; R. S. Chivukula, D. A. Dicus, H. J. He, S. Nandi, Phys. Lett. B **562** (2003) 109 [hep-ph/0302263]; Y. Abe *et al.*, Prog. Theor. Phys. **109** (2003) 831 [hep-th/0302115]; C. Csaki *et al.*, hep-ph/0305237; C. Csaki, C. Grojean, L. Pilo, J. Terning, hep-ph/0308038; Y. Nomura, JHEP **0311** (2003) 050 [hep-ph/0309189]; G. Burdman, Y. Nomura, hep-ph/0312247; C. Csaki *et al.*, hep-ph/0310355; R. Barbieri, A. Pomarol, R. Rattazzi, hep-ph/0310285.
- [14] R. Barbieri *et al.*, Phys. Rev. D **66** (2002) 024025 [hep-th/0203039]; S. Groot Nibbelink, H. P. Nilles, M. Olechowski, Phys. Lett. B **536** (2002) 270 [hep-th/0203055].
- [15] H. M. Lee, H. P. Nilles, M. Zucker, hep-th/0309195.
- [16] A. Hebecker, J. March-Russell, Nucl. Phys. B **625** (2002) 128 [hep-ph/0107039].
- [17] Y. Hosotani, Phys. Lett. B **126** (1983) 309; Phys. Lett. B **129** (1983) 193; Ann. Phys. **190** (1989) 233.
- [18] L. J. Dixon, J. A. Harvey, C. Vafa, E. Witten, Nucl. Phys. B **261** (1985) 678; *ibid.* **274** (1986) 285.
- [19] G. von Gersdorff, N. Irges, M. Quiros, hep-ph/0206029.
- [20] H. Georgi, A. K. Grant, G. Hailu, Phys. Lett. B **506** (2001) 207 [hep-ph/0012379].

- [21] C. A. Scrucca, M. Serone, L. Silvestrini, F. Zwirner, Phys. Lett. B **525** (2002) 169 [hep-th/0110073].
- [22] C. A. Scrucca, M. Serone, Nucl. Phys. B **564** (2000) 555 [hep-th/9907112].
- [23] D. M. Ghilencea, S. Groot Nibbelink, H. P. Nilles, Nucl. Phys. B **619** (2001) 385 [hep-th/0108184].
- [24] S. Groot Nibbelink, H. P. Nilles, M. Olechowski, M. G. A. Walter, Nucl. Phys. B **665** (2003) 236 [hep-th/0303101]; S. Groot Nibbelink, M. Laidlaw, hep-th/0311013, hep-th/0311015.
- [25] Z. Chacko, M. A. Luty, E. Ponton, JHEP **0007** (2000) 036 [hep-ph/9909248].